VOL. 18, NO. 3, FEBRUARY 2023 ISSN 1819-6608
ARPN Journal of Engineering and Applied Sciences

www.arpnjournals.com

EFFECT OF SURFACE COATING ON CHANGES IN MASS AND HEAT RATE ON HYDROPHOBIC LAYER COATED METAL FOAM

Syahrul Humaidi[1], Dahniar Hasibuan[1], Doli Bonardo[1], Fitri H. S. Ginting[1], Ayu Y. Sari[2], Lukman F. Nurdiyansah[2], Nining S. Asri[2], Eko A. Setiadi[2], Anggito P. Tetuko[2], Pardamean Sebayang[2], Achmad Maulana Soehada[3] and Nazaruddin Sinaga[4]
[1]Program (Physics), FMIPA, Universitas Sumatera Utara, Jln Bioteknologi, Indonesia
[2]Research Center for Advanced Materials, National Research and Innovation Agencey (BRIN), Tangerang Selatan, Banten, Indonesia
[3]Department of Physics, Universitras Sutomo, Serang, Banten, Indonesia
[4]Department of Mechanical Engineering, Faculty of Engineering, Diponegoro University, Semarang, Central Java, Indonesia
E-Mail: syahrul1@usu.ac.id

ABSTRACTS

The effect of hydrophobic coating on the surface of metal foam 15 pores per inch (PPI) on its basic thermal properties has been successfully analyzed. In addition, the characteristics of untreated metal foam have also been identified through 3-D optical microscope observations, surface morphology, and analytical models of capillary pressure. Metal foam 15 PPI has an average pore diameter of 746.7 m with a fairly even pore size distribution. The surface structure of the ligament is relatively rough with a fairly dense level of density. The super hydrophilic characteristics of metal foam can increase its capillary pressure. The hydrophobic layer on the metal foam surface did not significantly affect the porous surface morphology of the sample. The stability of metal foam in maintaining its intrinsic properties is relatively optimal, metal foam-based wick structure also has good thermal properties.

Keyword: coating, hydrophobic, metal foam, thermal, wick structure.

1. INTRODUCTION

In the last two decades, thermal management problems in electronic components have become the reason for the creation of heat-conducting and absorbing elements that can be applied in the fields of electronics and mechanics. The heat pipe is a breakthrough that is quite familiar in the industrial world in dealing with the problem of excessive heat transfer in various electronic components. This device allows the absorption of heat as well as cooling at hot points. The existence of a heat pipe as a two-phase heat transfer device is currently receiving considerable attention because it is an effective component to overcome various existing thermal management problems [Huang *et al*., 2017; Jafari *et al.,* 2017; Lee*et al.,* Ariantara *et al.,* Wits and Riele, 2017].

The heat pipe has three important components, namely the container, the working fluid [Asri, 2021]and the wick structure. The wick structure component plays an important role in ensuring capillary movement or fluid circulation during the effective performance of the heat pipe [Ginting, 2022], so this component needs to be further developed to maximize the overall performance of the heat pipe. This component will determine the start-up and thermal performance of the heat pipe. Thus, the different types of wick structures used will result in different heat transfer characteristics in the heat pipe. Various methods of making wick structures have been carried out, such as sintered metal powder, screen mesh, composite wicks, and groove wicks.

Currently, metal foam material has become one of the materials that have attracted the attention of researchers around the world because of its superiority in delivering heat energy [Chen *et al.*, 2020], due to its pore characteristics that support the accelerated transfer of thermal energy. When viewed from the material characteristics and physical properties, the structural wick material must meet several criteria that support the optimization of the thermal performance of the heat pipe. It must have a uniform pore size distribution with high porosity, stable crystalline structure, and hydrophilic properties on the surface to support the distribution of the working fluid in the wick structure in heat pipe applications.

In this work, we analyzed the material characteristics and analytical model of the capillary pressure of metal foam 15 PPI comprehensively to determine the functionality of metal foam as a wick structure in heat pipe applications. In addition, the hydrophobic liquid was used to coat the surface of the metal foam in order to investigate its effect on changes in mass and heat rate of metal foam on temperature dynamics.

2. METHODS

Metal foam samples were cut into rectangles with a length of 32.7 mm, a width of 8.2 mm, and a height of 7.3 mm as many as 3 pieces. Then the surface of the sample was smoothed with sandpaper, after which it was immersed in acetone for 20 minutes. Then, the sample was removed using tweezers that had been soaked in acetone liquid in another container to ensure it was not contaminated with any substances. After that, it was placed in a cup and put in the oven to be heated at 110 °C for 15 minutes and cooled in the oven until it reached room temperature (26°C). The characterization of the material and physical properties of the samples in this study included the distribution of pore diameter, porosity, surface morphology, and the ideal capillary pressure model. The thermal properties of metal foam were analyzed by previously treating it in the form of the

hydrophobic liquid coating on the surface of the metal foam to determine its effect on changes in mass and heat rate.

3. RESULTS AND DISCUSSIONS

3.1. 3-D Optical Microscope

Figures 1a and 1b show a 3-dimensional image of the 15 PPI metal foam morphology structure and the pore diameter distribution curve, respectively. As can be seen, the pores of the metal foam are spread fairly evenly with various size patterns. Normal pore diameter distribution graph with an average

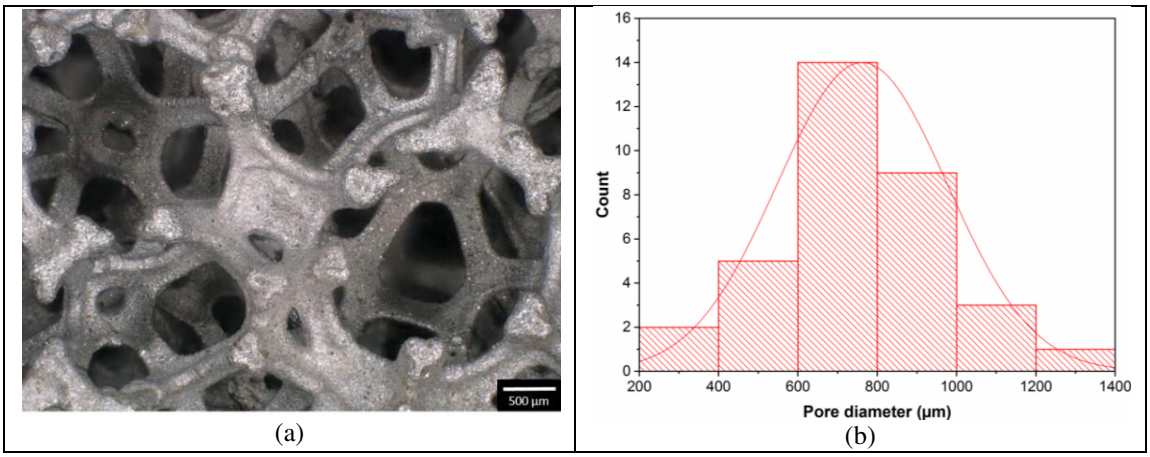

(a) (b)

Figure-1. 3-dimensional image of metal foam morphology (a) and metal foam pore diameter distribution (b).

pore diameter of 762 µm and dominated by pores with a diameter range of 600-800 µm. The results of the porosity measurement obtained a value of 45.2%, this means that the fraction of solids contained in the metal foam is 54.8%. Thus, the pore size is large enough to slow down the capillary pressure [Li *et al.,* 2018]. As such, it can slow down the rate of the working fluid when applied as a structural wick in a heat pipe.

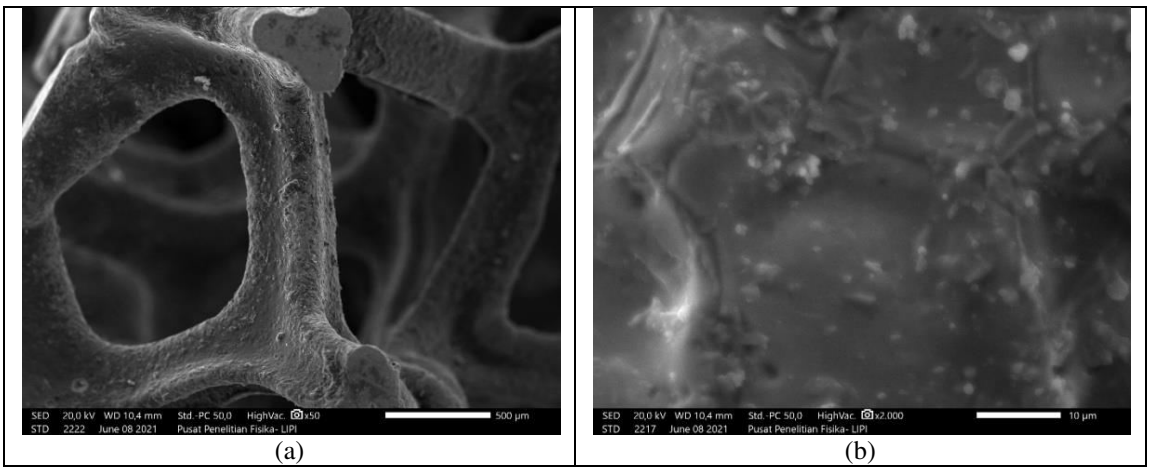

(a) (b)

Figure-2. SEM image of metal foam with magnification of 50 times (a) and 2000 times (b).

Figures 2. a and 2. b show SEM images of 30 PPI metal foam samples at 50 and 2000 times magnification. The solid structure of metal foam ligaments is shaped as three wires joined together. The surface of the ligament looks rough with granules scattered evenly on its surface. Cleaning using acetone causes an increase in the surface adhesiveness of metal foam to water [Sembiring *et al.,* 2021], this is because acetone can significantly improve wet ability performance [Zhong*et al.,* 2021]. This indicates that the ability of a liquid to maintain contact with a metal foam surface is relatively optimal [Ningrum *et al.,* 2022], and it is controlled by the balance between the intermolecular interactions of the adhesive type (liquid to surface) and cohesive type (liquid to liquid) [Moldoveanu and David, 2017].

3.2 Analytical Model of Metal Foam's Capillary Pressure

The ideal capillary pressure that can be achieved by metal foam is around 15 PPI, the analytical model is theoretically based on the concept of surface tension of water and the porosity of metal foam. The theoretical model is calculated using equation 1. The surface tension of water is symbolized by γ with a value of 72 dyne/cm, *r* is the metal foam pore radius of 15 PPI, and θ is the contact angle.

$$p_c = \frac{2\gamma \cos\theta}{r} \quad (1)$$

The contact angle is a criterion for perfect wetting on the metal foam surface. This characteristic is referred to as super hydrophilic, and material with these properties is very suitable to be applied as a wick structure material in heat pipes to increase its thermal performance [Guo, 2020; Ahmad*et al.,* 2018].

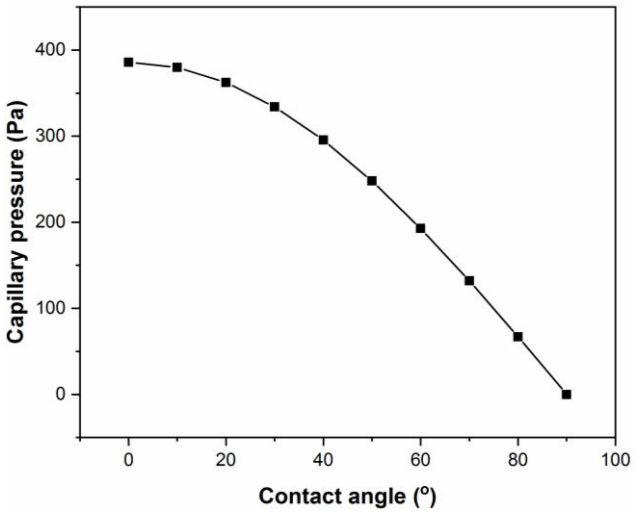

Figure-3. Graph of the relationship between metal foam contact angle and capillary pressure.

Figure-3 shows the relationship between the capillary pressure on the metal foam and the contact angle. Based on the analytical model, the optimum capillary pressure is obtained when the contact angle between the fluid and the pore surface is 0°.

A study to determine the relationship between the temperature of the metal foam sample and the indication of the change in mass of the metal foam was carried out using a thermogravimetric analysis (TGA) technique. This analysis will produce a percentage increase or decrease in mass when the sample without treatment and with the hydrophobic layer has an increase in temperature. Figure-4 shows a graph of the change in the mass of the sample with respect to its temperature. From the figure, both samples have experienced significant degradation after a temperature of 25.5 °C. But when viewed in detail through measurements, the decrease that occurs is only 0.31% for samples without a hydrophobic layer and 0.2873% for samples with a hydrophobic layer. Even the total mass change that occurred in the two samples did not reach 5%, however, the sample with the hydrophobic layer had the smallest mass change so the thermal stability was higher than the sample without the hydrophobic layer [Wang *et al.,* 2018*;* Dai *et al*., 2019].

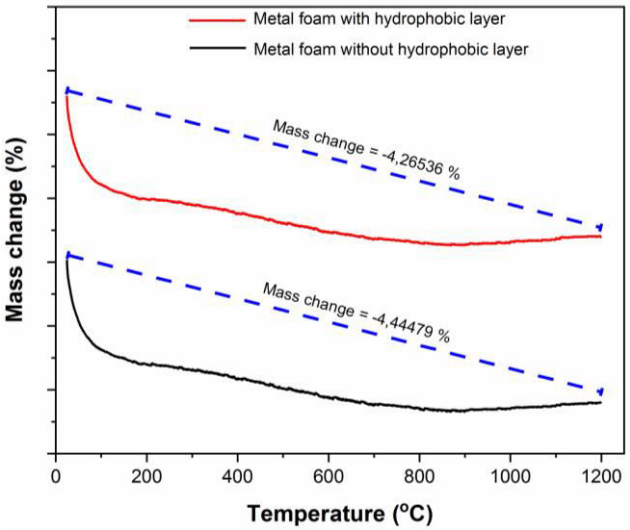

Figure-4. The relationship between temperature and mass changes in samples without hydrophobic layer and samples with hydrophobic layer.

The stability of the mass of metal foam against temperature dynamics occurs due to the absence of aromatic chains and volatile gases that make up the composition of metal foam. If the aromatic chain is one of the building blocks of metal foam, then the increase in temperature will cause the decomposition of the material in the form of breaking the aromatic chain [Lyu *et al*., 2019]. In addition, the carbon group will also experience carbonation when the temperature increases so that it will turn into carbon dioxide or carbon monoxide. Metal foam, which mainly contains metallic minerals, has a high melting point. This condition allows the metal foam to maintain its mass stability as the temperature increases to a certain extent.

3.3 DSC Analysis

In determining the relationship between temperature dynamics and the rate of heat that occurs in metal foam as a technique to analyze its thermal properties, a differential scanning calorimetry (DSC) test is carried out. This analysis will result in the rate of heat that occurs until it reaches its peak and then undergoes saturation, which means the heat rate has reached equilibrium when the sample without a hydrophobic layer and with a hydrophobic layer experiences an increase in temperature. The DSC curve will show the rate of heat flowing and form the thermal characteristics of the sample with respect to its temperature. Figure-5 shows the curve of the relationship between the heat rate and a given temperature from room temperature (23.7 °C) to a temperature of 1195.6 °C. Metal foam before and after

being coated with a hydrophobic layer showed 1 sloping peak or not too sharp. The peaks obtained indicate a change in the solid phase to liquid or solid-liquid phase change because it occurs at high temperatures between 600°C - 800°C[Zhang *et al*., 2018]. The untreated sample and the sample with a hydrophobic layer had melting points of 718 °C and 692 °C, respectively.

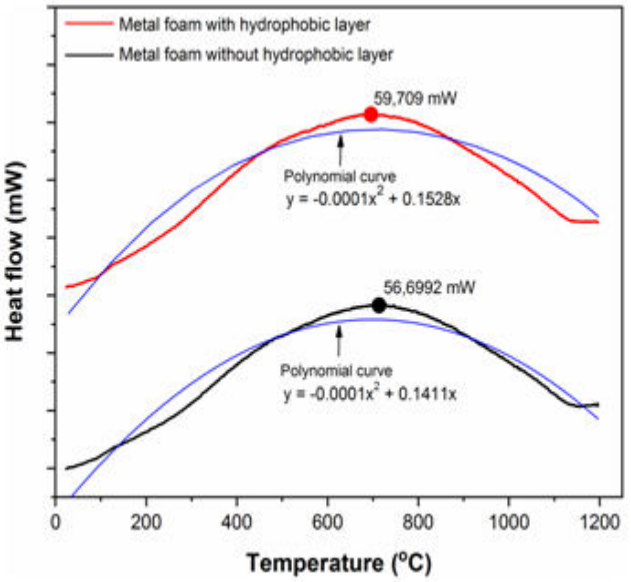

Figure-5. The relationship between temperature and heat rate in samples without hydrophobic layer and samples with hydrophobic layer.

The curve also shows a graph of polynomial equations to predict the value of the heat rate of metal foam samples to the increase in temperature that occurs. The y-axis represents the heat rate, while the x-axis represents the temperature which is substituted to determine the rate of heat that occurs so that at a certain temperature, the heat distribution of metal foam can be estimated numerically without initial testing. In each graph that is formed on samples without a hydrophobic layer and with a hydrophobic layer, the decrease in the curve does not reach the starting point so it shows semi-irreversible properties or cannot return to its original state, so metal foam has a melting point that needs to be avoided in order to remain stable in retaining its intrinsic properties.

4. CONCLUSIONS

In conclusion, the 15 PPI metal foam has a relatively low porosity below 50%, but the capillary pressure can be improved by increasing the wettability of the metal foam. Cleaning with acetone can increase the wettability of metal foam; this can be a new insight into the use of acetone as a working fluid to increase its capillarity rate so that it can improve the performance of structural wicks in heat pipe applications. The hydrophobic layer on the metal foam surface did not significantly affect the change in mass and heat rate because there was no chain reaction between metal foam solid particles and the hydrophobic liquid which caused mass degradation.

ACKNOWLEDGMENT

The authors would like to thank the laboratory of The Research Center for Advanced Material, National Research and Innovation Agency (BRIN) for the facilities used in this research. The authors would also thank the deputy of Engineering Sciences, National Research and Innovation Agency (BRIN) for the funding to support this research.

AUTHORS' NOTE

The authors declare that there is no conflict of interest regarding the publication of this article. The authors confirmed that the paper was free of plagiarism.

REFERENCES

Huang G., Yuan W., Tang Y., Zhang B., Zhang S. and Lu L. 2017. Exp. Therm. Fluid Sci. 82, 212-221.

Jafari D., Di Marco P., Filippeschi S. and Franco A. 2017. Exp. Therm. Fluid Sci. 88, 111-123.

Lee K. L., Kadambi J. R. and Kamotani Y. 2017. Int. J. Heat Mass Transf. 110, 496-505.

Ariantara B., Putra N. and Supriadi S. 2018. IOP Conf. Ser. Earth Environ. Sci. 105, 012045.

Wits W. W. and Riele G. J. 2017. Heat Mass Transf. 53, 3341-3351.

Asri N. S., Tetuko A. P., Esmawan A., Addin M., Setiadi E. A., Putri W. B. K., Ginting M. and Sebayang P. 2021. Nano-Structures & Nano-Objects 25, 100654.

Ginting F. H. S., Humaidi S. and Tetuko A. P. 2022. J. Phys. Conf. Ser. 2193, 012025.

Chen T., Shu G., Tian H., Zhao T., Zhang H. and Zhang Z. 2020. Appl. Energy 266, 114875.

Li H., Fu S., Li G., Fu T., Zhou R., Tang Y., Tang B., Deng Y. and Zhou G. 2018. Appl. Therm. Eng. 143, 621-629.

Sembiring E., Bonardo D., Sembiring K. and Sitorus Z. 2021. J. Phys. Conf. Ser. 2019, 012066.

Zhong G., Tang Y., Ding X., Chen G. and Li Z. 2021. Int. J. Heat Mass Transf. 179, 121642.

Ningrum R. A., Humaidi S., Sihotang S., Bonardo D. and Estananto J. 2022. Phys. Conf. Ser. 2193, 012009.

Moldoveanu S. C. and V. David V. 2017. in Sel. HPLC Method Chem. Anal. (Elsevier, pp. 279-328.

Guo H., Ji X. and Xu J. 2020. Int. J. Therm. Sci. 156, 106466.

Ahmad D., van den Boogaert I., Miller J., Presswell R. and H. Jouhara. 2018. Energy Sources, Part A Recover. Util. Environ. Eff. 40, 2686-2725.

Wang H., He M., Liu H. and Guan Y. 2019. ACS Appl. Mater. Interfaces. 11, 25586-25594.

Dai X., Shi L. and Qian W. 2019. J. Therm. Sci. 28, 597-607.

Lyu J., Wan Y., Wang N., Song Z., Liu Z. and Peng J. 2022. JCIS Open 5, 100041.

Zhang N., Yuan Y., Cao X., Du Y., Zhang Z. and Gui Y. 2018. Adv. Eng. Mater. 20, 1700753.